Mon. Not. R. astr. Soc. (1990) **245**, 713–719

Time-dependent dynamics of a planar galaxy model

S. Sridhar★
Raman Research Institute, Bangalore – 560 080 and Joint Astronomy Programme, Indian Institute of Science, Bangalore – 560012, India

R. Nityananda
Raman Research Institute, Bangalore – 5600 080, India

Accepted 1990 March 19. Received 1990 March 14; in original form 1989 December 29

SUMMARY

Time-dependent models of collisionless stellar systems with harmonic potentials allowing for an essentially exact analytic description have recently been described. These include oscillating spheres and spheroids. This paper extends the analysis to time-dependent elliptic discs. Although restricted to two space dimensions, the systems are richer in that their parameters form a 10-dimensional phase space (in contrast to six for the earlier models). Apart from total energy and angular momentum, two additional conserved quantities emerge naturally. These can be chosen as the areas of extremal sections of the ellipsoidal region of phase space occupied by the system (their product gives the conserved volume). The present paper describes the construction of these models. An application to a tidal encounter is given which allows one to go beyond the impulse approximation and demonstrates the effects of rotation of the perturbed system on energy and angular-momentum transfer. The angular-momentum transfer is shown to scale inversely as the cube of the encounter velocity for an initial configuration of the perturbed galaxy with zero quadrupole moment.

1 INTRODUCTION

Collisionless stellar systems are modelled by the collisionless Boltzmann equation (CBE) whose time-independent solutions are relatively well explored (e.g. the text by Binney & Tremaine 1987, hereafter BT), but time-dependent behaviour is less well understood. Large-scale numerical experiments have recently been carried out (e.g. Barnes 1989). It is possible that exact analytical solutions have some role to play in understanding the time-dependent behaviour of stellar systems and this paper is concerned with these. An early solution, due to Kalnajs (1973), describes a slab of uniform density executing homologous oscillations. Sridhar (1989) rederived this solution using constants of motion for time-dependent harmonic oscillators discussed by Lewis (1968). This method allowed the construction of uniform density oscillating spheres (Sridhar 1989) and also spheroids (Sridhar & Nityananda 1989, hereafter SN) with interesting coupled dynamics for the two independent axes. The equations governing the parameters of the spheres and spheroids had earlier been obtained from the virial theorem by Chandrasekhar & Elbert (1972) and Som Sunder & Kochhar (1986), respectively, but only on presupposing the existence of an underlying distribution function realizing the assumption of homologous oscillations.

This paper presents a model planar stellar system which is the logical time-dependent generalization of a static elliptic disc described by Freeman (1966) and is hence termed a generalized Freeman disc (GFD). A simple generalization would be along the lines suggested in SN and would give a disc with a and b varying in magnitude but fixed in direction. The model described in Section 2 of this paper is more general because, in addition, the directions of the principal axes change with time and the mean velocity field has internal circulation. This is, of course, remniscent of Freeman's (1966) analytic bars which are in fact a particular case stationary in a rotating frame. Section 2 also gives the detailed equations governing the time evolution of the 10 parameters which describe a GFD of a given mass. These parameters can be chosen as the 10 averages of products of phase-space variables, e.g. $\overline{x^2}$, $\overline{xv_y}$ etc. The general structure of the equations requires a quadratic potential which can include both the self-consistent potential of the disc and any external potential due to a perturber in the lowest tidal approximation. Even with the external time-dependent and non-axisymmetric potential, there are two conserved quantities. One is related to Liouville's theorem (invariant

★ Present address: Theoretical Astrophysics Group, Tata Institute of Fundamental Research, Homi Bhabha Road, Bombay 400 005, India.

phase volumes) and the other to Poincaré's invariant (a suitably defined area of a closed curve in phase space). Section 3 is a brief discussion of these general properties.

Section 4 sets up the problem of a GFD undergoing a tidal encounter. A point-mass perturber is chosen for simplicity. Explicit formulae for energy transfer in the impulse approximation are derived. These are compared with numerical integrations of the exact equations in Section 5. The behaviour of co- and counter-rotating systems is drastically different. Angular-momentum transfer which is zero in the impulse approximation can be explicitly calculated. The numerical scheme used is described in the Appendix.

2 KINEMATICS AND DYNAMICS OF A GENERALIZED FREEMAN DISC (GFD)

We define a GFD by the following distribution function:

$$\begin{aligned} f &= f_0(1-I)^{-1/2} && \text{for } I<1 \\ &= 0 && \text{for } I>1. \end{aligned} \tag{1}$$

The quantity I is a positive definite quadratic form in the four phase-space variables which we compress into a column vector for convenience:

$$\mathbf{z}=(x, y, v_x, v_y)^T. \tag{2}$$

We write I in terms of the associated real symmetric 4×4 matrix $\mathbf{Q}$:

$$I=\Sigma Q_{ij} z_i z_j \equiv \mathbf{z}^T\mathbf{Q}\mathbf{z}. \tag{3}$$

Essentially, the stars occupy an ellipsoidal region of phase space with level surfaces of the phase density on concentric similar ellipsoids. This projects down to an ellipse on the x–y plane. In what follows, we will need the phase-space averages of products like $z_i z_j$, since the energy, angular momentum and shape in real space can all be expressed in terms of these. A straightforward calculation shows that these second-order moments are directly given by the elements of $\mathbf{P}$, the matrix inverse to $\mathbf{Q}$:

$$\overline{z_i z_j}=\frac{1}{M}\int f_0(1-I)^{-1/2} z_i z_j\, dz = \tfrac{1}{5} P_{ij}.$$

One can also choose the 10 parameters differently to bring out their physical meaning. The shape clearly requires three parameters (major axis, minor axis, orientation), while the streaming motions require four parameters (two components of shear, expansion, and rotation). The peculiar velocities are again described in terms of three parameters defining an ellipse in velocity space.

The real space-surface density $\Sigma(x, y)$ is obtained by integrating out the velocities and takes the form

$$\Sigma(x, y)=\Sigma_0(1-q)^{1/2}, \tag{4}$$

where q is a positive definite quadratic form in x and y. The density is constant on the ellipses $q=$ constant (<1), and in a suitable coordinate system could be written as

$$\Sigma(x, y)=\frac{3M}{2\pi ab}\left(1-\frac{x^2}{a^2}-\frac{y^2}{b^2}\right)^{1/2}, \tag{5}$$

with M the total mass and axes a and b. The models given by Freeman have distribution functions which are particular cases of (1) and surface density (5), justifying the term GFD. The corresponding potential is quadratic in x and y within the ellipse and in the plane (the only region occupied by the stars)

$$\varphi(x, y)=\tfrac{1}{2} A^2 x^2+\tfrac{1}{2} B^2 y^2. \tag{6}$$

The force constants A^2 and B^2 are expressed in terms of the axis ratio parametrized by

$$k^2=1-b^2/a^2 \tag{7}$$

$$A^2=\frac{3GM}{k^2 a^3}[F(k)-E(k)] \tag{8}$$

$$B^2=\frac{3GM}{k^2 ab^2}[E(k)-(1-k^2)F(k)]. \tag{9}$$

E and F denote the two kinds of complete elliptic integrals defined by

$$E(k)=\int_0^{\pi/2}(1-k^2\sin^2\eta)^{1/2}\, d\eta \tag{10}$$

$$F(k)=\int_0^{\pi/2}(1-k^2\sin^2\eta)^{-1/2}\, d\eta. \tag{11}$$

In a general coordinate system making an angle θ to the principal axes, the potential takes the form

$$\varphi(x, y)=\tfrac{1}{2}\alpha x^2+\beta xy+\tfrac{1}{2}\gamma y^2, \tag{12}$$

with

$$\begin{aligned} \alpha &= A^2\cos^2\theta+B^2\sin^2\theta \\ \beta &= (A^2-B^2)\sin\theta\cos\theta \\ \gamma &= A^2\sin^2\theta+B^2\cos^2\theta. \end{aligned} \tag{13}$$

The angle θ and the axes a and b are easily expressed in terms of moments $\overline{x^2}$, $\overline{xy}$ and $\overline{y^2}$, i.e. P_{11}, P_{12} and P_{22},

$$\tan 2\theta = 2P_{12}/(P_{11}-P_{22})$$

$$a^2 = P_{11}\cos^2\theta+P_{12}\sin 2\theta+P_{22}\sin^2\theta$$

$$b^2 = P_{11}\sin^2\theta-P_{12}\sin 2\theta+P_{22}\cos^2\theta.$$

The accelerations are then given by

$$\begin{pmatrix}\dot v_x\\ \dot v_y\end{pmatrix}=-\begin{pmatrix}\alpha & \beta\\ \beta & \gamma\end{pmatrix}\begin{pmatrix}x\\ y\end{pmatrix}\equiv-\mathbf{F}\begin{pmatrix}x\\ y\end{pmatrix}, \tag{14}$$

where the real symmetric restoring force matrix $\mathbf{F}$ has been defined for convenience.

Combining (14) with $\dot x=v_x$, $\dot y=v_y$, we get the following matrix form for the equations of motion of a star

$$\frac{d\mathbf{z}}{dt}=\mathbf{K}\mathbf{z}, \tag{15}$$

where

$$\mathbf{K}=\begin{pmatrix}\mathbf{0} & \mathbf{1}\\ -\mathbf{F} & \mathbf{0}\end{pmatrix}. \tag{16}$$

We have written **K** in terms of 2×2 blocks and the restoring force **F** is given by (7)–(13).

Coming back to the original distribution function (1), it is necessary that f and hence I be invariant along phase trajectories (Jeans' theorem) so that the CBE is satisfied. We regard the elements of the matrix **Q** as functions of time, with evolution so chosen that I is invariant. This gives the condition

$$\frac{dI}{dt}=\sum_{ij}\frac{dQ_{ij}}{dt}z_iz_j+\sum_{ijl}Q_{ij}K_{il}z_iz_j+Q_{ij}K_{jl}z_jz_i \qquad (17)$$

$$=0$$

for all **z**.

We therefore have the matrix equation

$$\frac{d\mathbf{Q}}{dt}=-\mathbf{K}^T\mathbf{Q}-\mathbf{Q}\mathbf{K}. \qquad (18)$$

Multiplying on both left and right by $\mathbf{Q}^{-1}$, we get the equivalent equations for **P**:

$$\frac{d\mathbf{P}}{dt}=\mathbf{K}\mathbf{P}+\mathbf{P}\mathbf{K}^T. \qquad (19)$$

Like the original CBE, (19) is non-linear because of self-consistency, since **K** contains **F** which depends on **P**. The application to a tidal encounter given in the Section 4 requires the addition of more terms to the force matrix **F** but does not otherwise change the argument just given. The GFD remains a GFD with parameters evolving according to (19).

3 SOME GENERAL PROPERTIES

As is clear from equation (15), the phase space variables undergo a linear transformation for infinitesimal and hence also finite time steps. This transformation is also canonical since it is generated by Hamilton's equations:

$$\mathbf{z}(t)=\mathbf{S}(t)\,\mathbf{z}(0). \qquad (20)$$

(The notions of classical mechanics used in this section are discussed in detail in several textbooks, e.g. Arnold 1978.) One way of characterizing such transformations is that they preserve the following 'Poincare integral' taken around a closed curve $J=\int\Sigma_i p_i\,dq_i$. An equivalent statement for linear transformations is that the matrix **S** must be symplectic, i.e. must satisfy the property

$$\mathbf{S}^T\boldsymbol{\beta}\mathbf{S}=\boldsymbol{\beta}, \qquad (21)$$

where

$$\boldsymbol{\beta}=\begin{pmatrix}\mathbf{0} & \mathbf{1}\\ -\mathbf{1} & \mathbf{0}\end{pmatrix} \qquad (22)$$

in 2×2 block form. The change in the matrix **Q** (or **P**) in a finite time required to keep I invariant is easily worked out, using $I=\mathbf{z}^T\mathbf{Q}\mathbf{z}$

$$\mathbf{Q}(t)=\mathbf{S}^{T-1}(t)\mathbf{Q}(0)\,\mathbf{S}^{-1}(t) \qquad (23)$$

$$\mathbf{P}(t)=\mathbf{S}(t)\,\mathbf{P}(0)\,\mathbf{S}^T(t). \qquad (24)$$

Since **S** has 10 parameters (in four variables) and so does **Q**, it might appear from (23) that one could reach any $\mathbf{Q}(t)$ from a given $\mathbf{Q}(0)$ by applying a suitable symplectic transformation $\mathbf{S}(t)$. This is not true because there are two conserved quantities C_1 and C_2 as can be verified using equations (21)–(24):

$$C_1=Tr(\mathbf{Q}\boldsymbol{\beta})^2$$
$$C_2=Tr(\mathbf{Q}\boldsymbol{\beta})^4. \qquad (25)$$

Higher even powers do not give independent quantities in four dimensions (by the Cayley–Hamilton theorem). These two conserved quantities can be interpreted geometrically. The boundary of the occupied region in phase space is an ellipsoid which remains one under the linear transformations of phase-space generated by a quadratic potential (self-generated plus external). The volume of this ellipsoid is conserved. In addition, the 'area' of any plane section [strictly speaking the sum of areas projected on to the x–v_x and y–v_y planes – see the expression J between equations (20) and (21)] is conserved. As an alternative to the constants C_1 and C_2, one could choose the areas of two extremal plane sections of the ellipsoid whose product is proportional to the volume. We now have the 10-dimensional GFD space divided into eight-dimensional regions labelled by C_1 and C_2. Within each such region, it is possible to define Poisson brackets and write the equation of motion for **P** in a Hamiltonian form. One can further exploit energy and angular-momentum conservation (if there are no external potentials). The Hamiltonian form does guarantee that the solutions for **P** cannot show relaxing behaviour. Static models are fixed points of this Hamiltonian while Freeman's analytic bars correspond to closed periodic orbits. The behaviour of an isolated GFD is an interesting topic in its own right to which we hope to return elsewhere. In this paper, we discuss the specific case of a tidal encounter.

4 INCLUDING THE TIDAL FIELD OF A PERTURBER

We recall (12) that the internal gravitational potential of a GFD can be written as

$$\varphi(x,y,t)=\frac{\alpha}{2}x^2+\beta xy+\frac{\gamma}{2}y^2,$$

where α, β and γ are time-dependent.

From (13) and (14),

$$\mathbf{F}=\begin{pmatrix}\alpha & \beta\\ \beta & \gamma\end{pmatrix}$$

$$\alpha=A^2\cos^2\theta+B^2\sin^2\theta$$
$$\beta=(A^2-B^2)\sin\theta\cos\theta$$
$$\gamma=A^2\sin^2\theta+B^2\cos^2\theta.$$

A (perturbing) galaxy moving in the plane of the GFD exerts tidal forces on it. When the variation of this tidal force over the size of the GFD can be well represented by the first-order tidal approximation, we note that the addition of these tidal forces to the self-gravity of the GFD preserves the linearity of the equations of motion (15). All we need to do is to add the 'strengths' of the time-dependent tidal force to α,

β and γ. The perturber could be the extended halo of another galaxy which is assumed to have a rigid density distribution, or it could be another GFD whose structure itself could be time-varying and coupled to the original GFD. Or again, for simplicity, the perturber could be a point mass moving in the plane of the GFD. In any case, the relative motion between the perturber and the GFD is determined by

$$\ddot{\mathbf{R}} = \begin{pmatrix} \text{acceleration of the} \\ \text{centre of mass of the} \\ \text{perturber by the GFD} \end{pmatrix} - \begin{pmatrix} \text{acceleration of the} \\ \text{centre of mass of the} \\ \text{GFD by the perturber} \end{pmatrix}, \quad (26)$$

where $\mathbf{R}$ is the separation between the centres of the perturber and the GFD. We note that (26) contains the back reaction of the GFD on the orbital motion and allows for energy and angular-momentum transfer from the orbital motions of the GFD and the perturber to the internal motions of stars within the GFD.

In particular, for a point-mass perturber, the addition of its tidal field changes

$$\mathbf{F} = \begin{pmatrix} \alpha & \beta \\ \beta & \gamma \end{pmatrix} \text{ to } \mathbf{F}' = \begin{pmatrix} \alpha' & \beta' \\ \beta' & \gamma' \end{pmatrix}, \quad (27)$$

where

$$\alpha' = \alpha - GM_2\left[\frac{3(\mathbf{R}\cdot\hat{\mathbf{x}})^2}{R^5} - \frac{1}{R^3}\right],$$

$$\beta' = \beta - 3GM_2\left[\frac{(\mathbf{R}\cdot\hat{\mathbf{x}})(\mathbf{R}\cdot\hat{\mathbf{y}})}{R^5}\right], \quad (28)$$

$$\gamma' = \gamma - GM_2\left[\frac{3(\mathbf{R}\cdot\hat{\mathbf{y}})^2}{R^5} - \frac{1}{R^3}\right].$$

The force exerted by the GFD on the point mass depends on the instantaneous shape, size and orientation of the GFD. However, to first order in (size/R), this force depends only on the position of the centre of mass of the GFD. So we write

$$\ddot{\mathbf{R}} = -\frac{G(M_1+M_2)}{R^3}\mathbf{R}, \quad (29)$$

where corrections are second order in $\left(\frac{\text{size of GFD}}{R}\right)$.

5 PRELIMINARY NUMERICAL STUDIES

We study the response of a GFD to a point mass moving in its plane by numerically integrating (19):

$\dot{\mathbf{P}} = \mathbf{K}'\mathbf{P} + \mathbf{P}\mathbf{K}'^T$.

$\mathbf{K}'$ now is given by

$$\mathbf{K}' = \begin{pmatrix} \mathbf{0} & \mathbf{1} \\ -\mathbf{F}' & \mathbf{0} \end{pmatrix}, \quad (30)$$

where $\mathbf{F}'$, which includes both the self-gravity of the GFD and the tidal force of the point mass, is given in (28). The motion of the point mass is governed by (29).

The formalism allows for cases in which the perturber moves along elliptic or circular trajectories around the GFD. In this preliminary study we shall, however, only consider cases when it describes a hyperbola. At time = 0 we keep the point mass far away [$R(0) > 50 \times$ GFD size] from the GFD and choose the GFD itself to be a Kalnajs' disc. This is a circular disc in which the ratio of rotational to pressure support can be varied. Let us recall the form of the phase-space distribution function of the Kalnajs' disc (BT),

$$F_K(E, L_z) = \left[\frac{3M}{4\pi^2 a^4(\Omega_0^2-\Omega^2)}\right]\left[1+\frac{2(\Omega L_z - E)}{a^2(\Omega_0^2-\Omega^2)}\right]^{-1/2}$$

$$= \left[\frac{3M}{4\pi^2 a^4(\Omega_0^2-\Omega^2)}\right]\left[1+\frac{(2\Omega r v_\theta - v_\theta^2 - v_r^2 - \Omega_0^2 r^2)}{a^2(\Omega_0^2-\Omega^2)}\right]^{-1/2}. \quad (31)$$

Using

$$\begin{pmatrix} v_r \\ v_\theta \end{pmatrix} = \begin{pmatrix} \cos\theta & \sin\theta \\ -\sin\theta & \cos\theta \end{pmatrix}\begin{pmatrix} v_x \\ v_y \end{pmatrix} \quad (32)$$

in (31), we can immediately write down the matrix $\mathbf{Q}_K$ as

$$\mathbf{Q}_K = \frac{1}{a^2(\Omega_0^2-\Omega^2)}\begin{pmatrix} \Omega_0^2\mathbf{1} & \Omega\mathbf{J} \\ -\Omega\mathbf{J} & \mathbf{1} \end{pmatrix}, \quad (33)$$

where

$$\mathbf{1} = \begin{pmatrix} 1 & 0 \\ 0 & 1 \end{pmatrix} \text{ and } \mathbf{J} = \begin{pmatrix} 0 & -1 \\ 1 & 0 \end{pmatrix}. \quad (34)$$

We can easily invert $\mathbf{Q}_K$ to get $\mathbf{P}_K = \mathbf{Q}_K^{-1}$:

$$P_K = \begin{pmatrix} a^2\mathbf{1} & -\Omega a^2\mathbf{J} \\ \Omega a^2\mathbf{J} & \Omega_0^2 a^2\mathbf{J} \end{pmatrix}. \quad (35)$$

Let the point-mass perturber pass by with a distance of closest approach = $s(\gg a)$ where its speed is v. Before we describe our results in the next section let us see what the impulse + tidal approximation predicts for the changes in energy and angular momentum of the disc.

5.1 Predictions of the impulse + tidal approximations

When the perturber moves so fast that the encounter time is significantly smaller than the orbital times for stars within a galaxy, the impulse approximation (Spitzer 1958) can be used to estimate changes in gross quantities like energy and angular momentum of the perturbed galaxy. Further, when the tidal field of the perturber can be well represented by the first-order tidal approximation, one obtains a simple and useful expression for the impulse given to a star at position $\mathbf{r}$ from the centre of the perturbed system (impulse, $\Delta\mathbf{v}$ = change in velocity relative to the perturbed galaxy).

Within the impulse approximation it is consistent to assume that the perturber moves in a straight line:

$$\mathbf{R}(t) = (s, vt, 0). \quad (36)$$

Then (see, e.g. BT),

$$\Delta\mathbf{v}(\mathbf{r}) \approx \frac{2GM_2}{s^2 v}(x, 0, -z) \quad (37)$$

from which the energy and angular momentum gained by the disc (which is described by the distribution function in equation 31) can be computed. The energy change of the Kalnajs' disc is

$$\Delta E_{\rm imp} = \frac{2G^2 M_2^2 M_1}{s^4 v^2}\,\overline{r^2}, \tag{38}$$

while the angular momentum of the disc remains unchanged in this approximation:

$$\Delta L_{\rm imp} = 0. \tag{39}$$

The total energy of the undisturbed Kalnajs' disc is

$$E = -\frac{M}{5}\,\Omega_0^2 a^2. \tag{40}$$

Defining dynamical time for the unperturbed disc $= t_{\rm dyn} = 1/\Omega_0$ and encounter time $= t_{\rm enc} = s/v$, we can write the fractional energy transfer as

$$\frac{\Delta E_{\rm imp}}{|E|} = \frac{32}{9\pi^2}\left(\frac{M_2}{M_{\rm disc}}\right)^2\left(\frac{t_{\rm enc}}{t_{\rm dyn}}\right)^2\left(\frac{a}{s}\right)^6. \tag{41}$$

These are the results in the impulse approximation, which can be compared to the exact calculation for this model described below.

At $t=0$ the system was chosen to be a Kalnajs' disc of unit mass and radius. The gravitational constant, G, was set equal to unity in all cases. Then $\Omega_0^2 = 3\pi/4$ and the only free disc parameter is Ω, the angular-rotation velocity. The kinetic and potential energies of the disc do not depend on Ω:

$$\begin{aligned}&\text{kinetic energy} = T = 3\pi/20,\\ &\text{potential energy } W = -2T = -3\pi/10,\end{aligned} \tag{42}$$

while the angular momentum (L) is proportional to Ω:

$$L = \frac{2\Omega}{5}. \tag{43}$$

The perturber was chosen to be a point mass with mass $M_2 = 2000$. It was set on a (Keplerian) hyperbolic trajectory with a distance of closest approach, $s = 20$. Since the perturber is on a hyperbolic trajectory, there is a certain maximum angle, $\phi_{\max}$, which its asymptotic velocity at $t=\infty$ makes with the line joining the centre of the disc and the point of closest approach:

$$\phi_{\max} = \cos^{-1}\left(\frac{1}{\text{eccentricity}}\right);\ \phi_{\max} > \pi/2 \tag{44}$$

for an unbounded orbit.

At $t=0$, the perturber was chosen to be at $(-0.9\,\phi_{\max})$. The speed at closest approach was varied from its minimum allowed value ($v_{\min} = [2G(M_1+M_2)/s]^{1/2} \approx 14.14$) – for parabolic orbits – to quite large values. The response of the disc was monitored by solving (30) numerically for a period of time in which the perturber moved from $\phi = -0.9\,\phi_{\max}$ to $\phi = +0.9\,\phi_{\max}$. The program that solves (30) numerically is described in the Appendix where now the tidal field of the perturber is also included.

We have performed numerical experiments for the cases $\Omega = +0.5, 0$ and -0.5. While the behaviour of the disc itself is an interesting problem that remains to be understood, we discuss here only the energy and angular-momentum changes. Using equations (40) and (41) we note that the (impulse plus tidal) approximation predicts

$$\frac{\Delta E_{\rm imp}}{|E|} = 0.0225158\left(\frac{1}{\tau^2}\right) \tag{45a}$$

$$\Delta L_{\rm imp} = 0, \tag{45b}$$

where

$$\tau = t_{\rm dyn}/t_{\rm enc} = v/s\Omega_0 \tag{45c}$$

is a dimensionless measure of v.

5.2 Energy and angular momentum transfer

Fig. 1 shows the results for the fractional energy transfer as a function of the parameter τ for three values of the angular velocity $\Omega = 0.5,\ 0,\ -0.5$. The ordinate Y (plotted on a log scale) has been defined as follows:

$$Y = \frac{\Delta E}{|E|}\,\tau^2. \tag{46}$$

The impulse approximation would predict $Y = Y_{\rm imp} = 0.022\,515\,8$ for all τ. The curves thus give a clear idea of deviations from impulsive behaviour. The parameter τ ranges from its minimum value $\tau_{\min}$ corresponding to a parabolic orbit $\tau_{\min} = v_{\min}/s\Omega_0 = 0.4608$ to about 2.5. It is clear that the results approach $Y_{\rm imp}$ for fast encounters, i.e. with

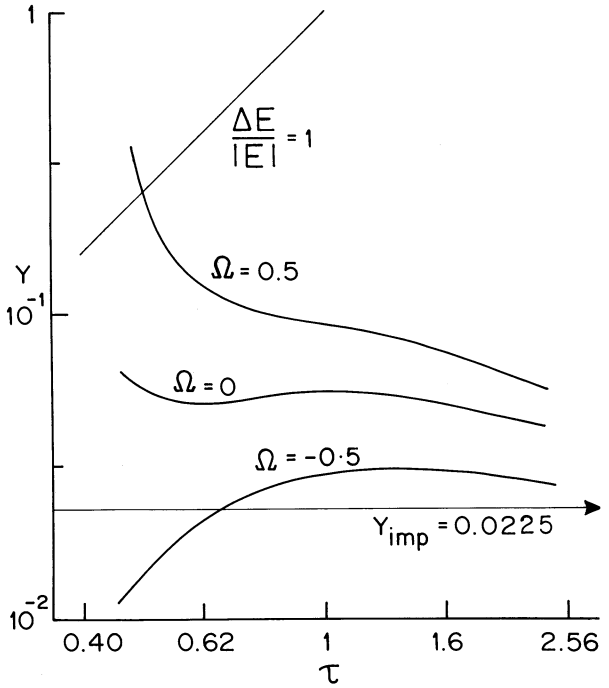

Figure 1. Deviations from the impulse approximation measured by Y (equation 46) as a function of the encounter speed measured by τ (equation 45c) for three Kalnajs' discs with angular velocities $\Omega = 0.5,\ 0,\ -0.5$. Note the line corresponding to disruption, i.e. $\Delta E/|E| = 1$, and the impulse limit $Y_{\rm imp} = 0.022\,515\,8$.

increasing τ. This is confirmed by simulations (not shown in Fig. 1) for much larger values of τ. The energy transfer is largest in the corotating case $\Omega = +0.5$, and in fact approaches the case of disruption $\Delta E/|E| = 1$ for the slowest encounters ($\tau \sim 0.5$). Even in this case, a check of parameters of the GFD confirms that the tidal approximation is still valid. The energy transfer in the counter-rotating case $\Omega = -0.5$ remains small and even goes below $Y_{\rm imp}$. This can be understood in qualitative terms – the tidal field of the perturber follows a good fraction of the stellar orbits only in the corotating case. The $\Omega = 0$ case is intermediate.

It should be mentioned that an isolated GFD showed energy and angular-momentum changes of less than 10^{-4}, showing that the numerical scheme was adequate. Another satisfying check was that the bar instability discussed by Kalnajs (1972) was shown in the simulations at around $\Omega = 0.75$ as expected (in fact the non-linear behaviour can be followed in this case). Fig. 2 shows the angular-momentum transfer as a function of τ in the same three cases, $\Omega = 0.5, 0, -0.5$. As before, the effects are largest in the co-rotating case, reaching ΔL of the same order as L ($= 0.2$ for $\Omega = 0.5$). The rather rapid onset of strong energy and angular-momentum transfer as the encounter becomes slower, reflects the increasing responsiveness of an already distended and elongated disc to further tidal forces/torques. This non-linear feedback effect (within the tidal approximation) is included self-consistently in the treatment given here and is illustrated in Fig. 3. The approximate τ^{-3} behaviour at large τ of the angular-momentum transfer ΔL (Fig. 2) is rather striking.

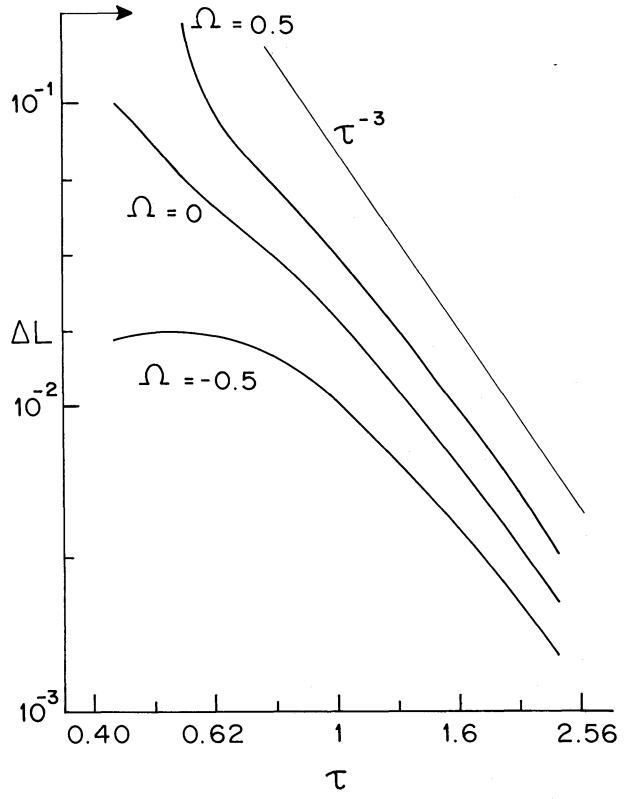

Figure 2. Angular-momentum transfer ΔL as a function of encounter speed τ for the same three cases as in Fig. 1. Note the approximate τ^{-3} decrease.

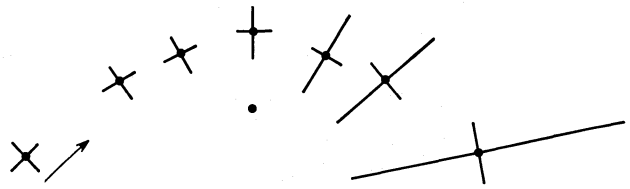

Figure 3. Variation of the galaxy shape during a strong encounter leading to disruption. The dimensions of the galaxy relative to those of its orbit have been exaggerated by a factor of 10. The parameters are $\tau = 0.49 (v = 5$ at infinity), $\Omega = 0.5$.

The following argument suggests that it is not unexpected. The impulse approximation neglects the movement of the stars during the encounter. Denoting the accelerations caused by the perturber by a, these displacements are of order $at_{\rm enc}^2$. (The larger displacements $v\Delta t$ caused by the unperturbed motions in the galaxy do not change its distribution function and can be ignored.) The perturbing torques act on this distortion for a time $t_{\rm enc}$, giving $\Delta L \sim t_{\rm enc}^3$, i.e. τ^{-3}.

6 DISCUSSION

In a different context, Subramanian (1989) considered the response of a maximally rotating Kalnajs' disc to the tidal field of a perturber (in the first-order tidal approximation) moving in its plane. The disc itself was assumed to be embedded in a rigid, homogeneous spherical halo. Such a halo introduces an additional potential $\phi_{\rm h} = \frac{1}{2}\Omega_{\rm h}^2(x^2 + y^2)$ which can be incorporated in the formalism we have used to describe GFDs. The Kalnajs' disc problem studied by Subramanian turns out to be a particular cold case of the interactions of GFDs discussed in this paper.

Palmer & Papaloizou (1982) studied the effect of a slow encounter on a rotating disc in an approximation that went beyond the impulse approximation, but one which neglected the changes in the self-gravity of the disc during the encounter. The present work goes beyond their analysis in that the fully self-consistent response of the GFD is retained, although we are restricted to harmonic potentials.

The formalism we have set up allows a wide range of interesting situations which are yet to be explored in full. Energy and angular-momentum transfer, heating, and disruption of a model galaxy by an encounter, can be studied. It should be mentioned that there is no post-encounter relaxation in this model. A more realistic model would presumably relax. However, some aspects of encounters involve behaviour on at most a few dynamical time-scales and we are optimistic that the model described in this paper will prove to be a useful guide to the behaviour of more realistic systems. For example, features like the range of validity of the impulse approximation, the nature and size of the corrections to it, and their scaling with encounter speed are likely to be robust.

The present models, being based on a harmonic potential, are characterized by a single time-scale that might make them exceptionally susceptible to disruption by tidal forces. More realistic models have a range of orbital time-scales present and, in these, only some orbits may undergo violent perturbations in a given encounter. This must be borne in mind when assessing the implications of the results presented in this paper.

REFERENCES

Arnold, V. I., 1978. *Mathematical Methods of Classical Mechanics,* Springer-Verlag, New York.
Barnes, J. E., 1989. *Nature,* **338,** 123.
Binney, J. & Tremaine, S., 1987. *Galactic Dynamics,* Princeton University Press.
Chandrasekhar, S. & Elbert, D. D., 1972. *Mon. Not. R. astr. Soc.,* **155,** 435.
Freeman, K. C., 1966. *Mon. Not. R. astr. Soc.,* **134,** 15.
Kalnajs, A. J., 1972. *Astrophys. J.,* **175,** 63.
Kalnajs, A. J., 1973. *Astrophys. J.,* **180,** 1023.
Lewis, H. R., 1968. *J. math. Phys.,* **9,** 1976.
Palmer, P. L. & Papaloizou, J., 1982. *Mon. Not. R. astr. Soc.,* **199,** 869.
Som Sunder, G. & Kochhar, R. K., 1986. *Mon. Not. R. astr. Soc.,* **221,** 553.
Spitzer, L., 1958. *Astrophys. J.,* **127,** 17.
Sridhar, S., 1989. *Mon. Not. R. astr. Soc.,* **238,** 1159.
Sridhar, S. & Nityananda, R., 1989. *J. Astrophys. Astr.,* **10,** 279 (SN).
Subramanian, K., 1989. *Mon. Not. R. astr. Soc.,* **238,** 1345.

APPENDIX: NUMERICAL SCHEME USED FOR GFDs

We outline the basic features of the numerical scheme used to solve equation (19) self-consistency. We recall that

$$\dot{\mathbf{P}} = \mathbf{KP} + \mathbf{PK}^T, \tag{A1}$$

where

$$\mathbf{K} = \begin{pmatrix} \mathbf{0} & \mathbf{1} \\ -\mathbf{F} & \mathbf{0} \end{pmatrix}. \tag{A2}$$

$\mathbf{F}$ is the 2×2 matrix given by equations (13) and (14). $\mathbf{F}$ depends on P_{11}, P_{12}, P_{22} and this is what makes (A1) nonlinear and self-consistent. When (A1) is to be solved numerically, one has to use a finite difference scheme. We use the 'finite' version of the evolution equations as given in (24)

$$\mathbf{P}(t_2) = \mathbf{SP}(t_1)\,\mathbf{S}^T, \tag{A3}$$

instead of writing down a naive finite difference approximation to (A1) itself. The advantage of evolving by (A3) is that symplectic properties (like conservation of C_1, C_2) are automatically preserved up to machine accuracy. $\mathbf{S}$ is that symplectic matrix which takes $\mathbf{z}(t_1)$ to $\mathbf{z}(t_2)$:

$$\mathbf{z}(t_2) = \mathbf{S}\mathbf{z}(t_1). \tag{A4}$$

This is just the evolution equation (in finite difference form) for two coupled harmonic oscillations. A simple leap-frog scheme (update coordinates and then momenta with forces computed from the new coordinates) will guarantee preservation of the symplectic nature of the equations as well as numerical accuracy to second order in Δt. The matrix that updates coordinates is

$$\mathbf{S}_x = \begin{pmatrix} \mathbf{1} & \Delta t\mathbf{1} \\ \mathbf{0} & \mathbf{1} \end{pmatrix}, \tag{A5}$$

while the matrix that updates momenta is

$$\mathbf{S}_v = \begin{pmatrix} \mathbf{1} & \mathbf{0} \\ -\Delta t\mathbf{F} & \mathbf{1} \end{pmatrix}. \tag{A6}$$

We write

$$\mathbf{S} = \mathbf{S}_{v1/2}(\overbrace{\mathbf{S}_x\mathbf{S}_v}^{1}\ldots\overbrace{\mathbf{S}_x\mathbf{S}_v}^{N})\,\mathbf{S}_{x1/2}, \tag{A7}$$

where the time interval $(t_2 - t_1)$ has been subdivided into N equal intervals,

$$\Delta t = (t_2 - t_1)/N. \tag{A7}$$

$\mathbf{S}_{x1/2}$ and $\mathbf{S}_{v1/2}$ are the updates over times $\Delta t/2$; this is required by any leap-frog scheme. Since we are dealing with a self-consistent problem, $\mathbf{S}_v$ at each stage is calculated from the current value of $\mathbf{P}$.

The addition of the tidal field of a perturber just adds terms to F and the whole scheme outlined above goes through.